Natural Resources Research, Vol. 21, No. 1, March 2012 (© 2012)
DOI: 10.1007/s11053-011-9166-9

Stream Sediments Geochemical Exploration in the Northwestern Part of Wadi Allaqi Area, South Eastern Desert, Egypt

Ahmed M. El-Makky[1,3] and Kadry N. Sediek[2]

Received 19 August 2011; accepted 12 December 2011
Published online: 4 January 2012

Geochemical stream sediments survey was conducted in the northwestern part of Wadi Allaqi area, Eastern Desert, Egypt. The area comprises Precambrian metasediments, intermediate metavolcanics, gabbro, and serpentinites, with intrusive masses of granites and quartz-porphyry and invaded by several quartz veins. The −1.0-mm size fraction is analyzed for As, Cu, S, Mo, Pb, Zn, Co, Ni, Rb, Ba, Sr, Nb, V, U, Th, Cr, Zr, La, Ce, Nd, and Y. The geochemical survey is supported by heavy minerals study in the −0.125 + 0.0625-mm fraction. The geochemical data were statistically investigated using Q-mode cluster and R-mode factor analyses as well as the enrichment factor. Factors 1 (Zr, Nb, Nd, La, and Y), 2 (V, Sr, and Zn), and 4 (Ba and Rb) are mainly controlled by the lithological characters of the rocks hosting Au-sulfide mineralizations and their accompanied hydrothermal alteration zones. In the mineralization Factor 3 (Cu, S, As, Ce, and Mo), arsenic, Cu, S, and Mo are direct indicators, while Ce is indirect one for the Au-sulfide mineralizations. The Cu–S–As–Mo association with Pb and Zn anomalies in the stream sediments draining the quartz-porphyry point to its porphyry copper mineralization. Cobalt and Ni (Factor 5) are pathfinders for the Fe- and Cu-sulfides, whereas Zn and Pb of Factor 8 are additional pathfinders for the Au-sulfide mineralizations. The southern stream sediments having high U/Th ratios with U–Mo association and draining granites traversed by pegmatites, as well as the stream sediments draining Um Garayat area and the quartz-porphyry stock with high abundance of monazite, zircon, epidote, sphene, and ilmenite, could signify sources of U and Th (Factor 7). Two watershed areas have distinct enrichment factors for arsenic suggesting unexplored extensions of Au-sulfide mineralization linked to the Allaqi shear-zone. The enrichment of the mineralization Factor 3 in the drainage system is mainly controlled by the prevailed mechanical dispersion for the hosting heavy minerals in such arid region with minor role of hydromorphic dispersion. The chemistry and mineralogy of the stream sediments are evidently allied to the drained bedrocks and their hosted mineralizations that signify a promising area for detailed exploration.

KEY WORDS: Allaqi shear zone, lithochemical drainage survey, statistical analyses, geochemical associations.

INTRODUCTION

The study area lies in the southeastern part of Egypt, distant about 200-km southeast of Aswan city (Fig. 1). This area has arid climatic nature (Cancer zone), where rarely rain falls and daily temperature exceed 45°C in summer and less than 20°C in winter. Occasionally, heavy rain falls in autumn season, which may form torrents pouring in the drainage system of Wadi Allaqi and the other nearby wadis such as Haimur. The topographic relief varies from moderate to low mountains. In general, Quaternary sediments of various sizes ranging from clay to gravel size fractions cover the wadis in the study area.

[1]Biological and Geological Sciences Department, Faculty of Education, Alexandria University, Soter, Alexandria, Egypt.
[2]Geology Department, Faculty of Science, Alexandria University, Alexandria, Egypt.
[3]To whom correspondence should be addressed; e-mail: ahmedelmakky@yahoo.com

1520-7439/12/0300-0095/0 © 2012 International Association for Mathematical Geology

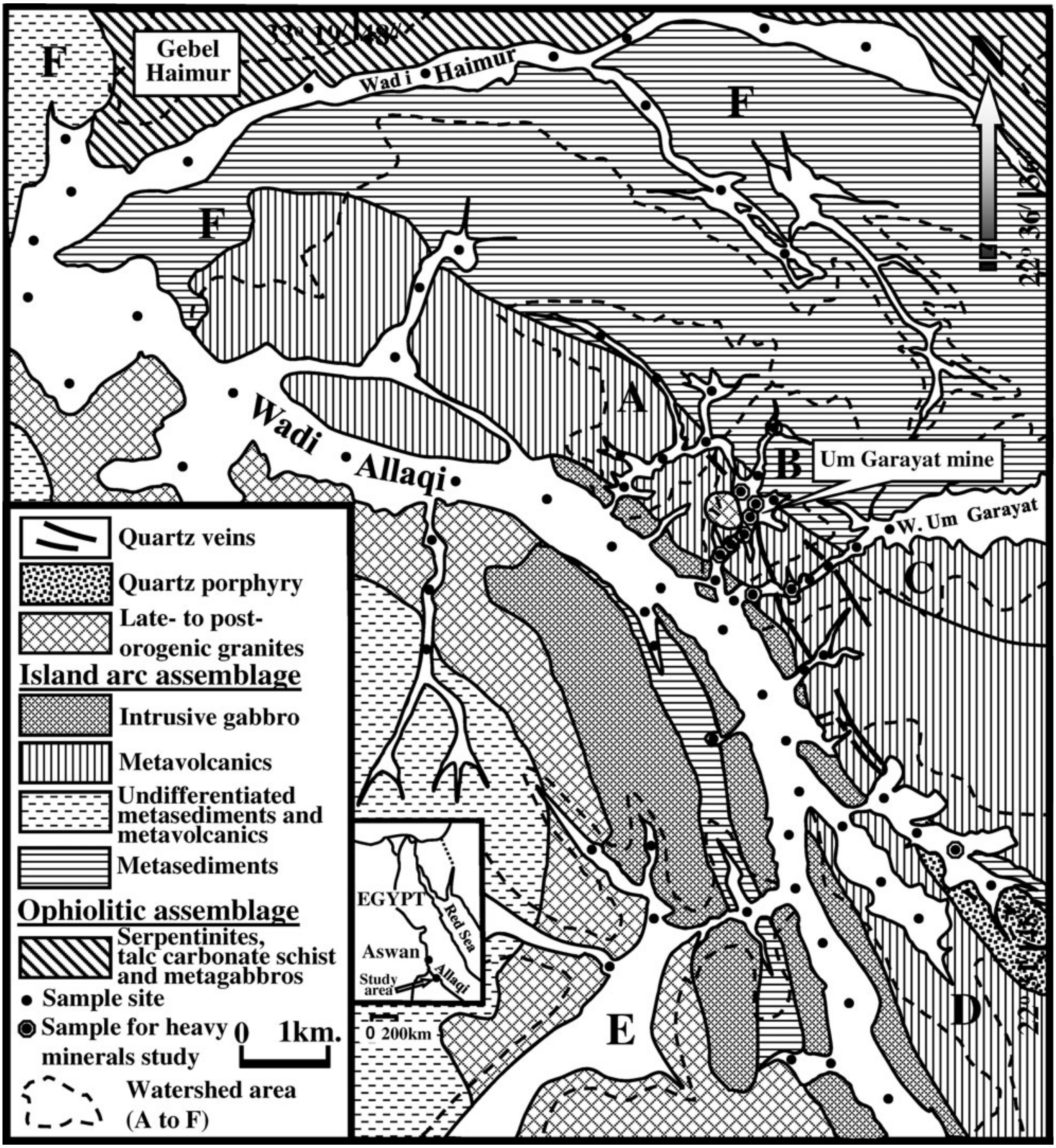

Figure 1. Geologic and sampling map of the northwestern part of Wadi Allaqi area, (modified after Hunting Geology and Geophysics Ltd 1967; Ivanov and Hussein 1972; El Nisr 1997; Ramadan et al. 2001; Darwish 2004).

The Wadi Allaqi area includes ca 17 gold occurrences, and had attracted the attention since the Pharaonic times; ancient Egyptians did especial stress on the prospecting and exploration especially for gold. The prospecting had activated through the Roman time and the early Islamic period. The early production of gold was from the alluvial sediments and exposed veins and later on from the underground veins (Afia and Imam 1979). At Um Garayat area, the geochemical studies (Ivanov 1988) have not led to re-opening the ancient mine. Recently, in 2004, the Australian GIPPSLAND Company carried out an exploration for Au, Cu, and Ni mineralizations in Wadi Allaqi region. In drill holes at Um Garayat area, the Au-content within the shear structures returned 2.17 g/t, whereas in Haimur area, the maximum Au-content within the regolith returned 6.91 g/t.

In the study area, Au- and Cu-Au mineralizations are located within the major complex Allaqi shear-zone, which extends from south Aswan city to the northern border of Sudan. These mineralizations are hosted mainly in the highly altered metavolcanics at Um Garayat area, and the quartz-porphyry stock at the southeastern part (Fig. 1). The mineralization is restricted to quartz veins, lenses, and adjacent wall-rock alteration zones including irregular silicified metasomatic bodies. The mineralized quartz veins, lenses, and silicified bodies are accompanied by apatite, tourmaline, and calcite (Ivanov 1988; Hussein 1990; El-Kazzaz 1996a). The types of alterations are propylitization, pyrophillitization, silicification, carbonatization, pyritization, alunitization, sericitization, albitization, and kaolinitization. Throughout three phases of hydrothermal stage, the ore minerals pyrite, pyrrhotite, chalcopyrite, native gold, Au-tellurides, and proustite were developed in addition to supergene covellite and chalcocite as well as widespread limonite (Ivanov 1988). At Haimur area in the northwestern part (Fig. 1), chalcopyrite, arsenian pyrite, sphalerite, and galena are associated with Au-bearing quartz and quartz-carbonate veins trending NE–-SW to ENE–WSW along shear zone and thrust fault plane accompanying with sericitization, silicification, sulfidization, and carbonatization (Darwish 2004).

The geochemical survey of sediments in drainage patterns is exceedingly effective during the prospecting for some metallic mineralizations in the arid conditions prevailing in the Eastern Desert of Egypt (e.g., Anwar et al. 1984; El Bouseily et al. 1985; Obeid et al. 2001). The main purpose of this article is to carry out explorative stream sediments geochemical survey to seek geochemical signatures and elucidating anomalous sites that may indicate some new gold extensions or other mineralizations and this may reveal the element associations in the primary mineralization.

GEOLOGICAL AND STRUCTURAL SETTINGS

The Wadi Allaqi district had attained several studies; Hunting Geology and Geophysics Ltd (1967) produced a generalized photogeological map (scale of 1:500,000) in which the rocks designated as geosynclinal metasedimentary and metavolcanic types. El Ramly (1972) assigned all the rocks to the geosynclinal Shadli meta-volcanic group, intruded by a metagabbro–diorite complex and granitoids. The Wadi Allaqi area is covered by several litho-tectonic metamorphic units of Late Proterozoic age. The rocks, which crop out in the Wadi Allaqi area have been affected by strong deformation and regional low-grade, greenschist-facies metamorphism, during the Pan-African orogeny (El-Kazzaz 1995; Rashwan et al. 1995; El-Kazzaz 1996b; El Kazzaz and Taylor 1996) and superimposed by hydrothermal alterations (Ivanov 1988; El Nisr 1997).

As cited by Ivanov (1988) and El Nisr (1997), the exposed Precambrian rocks in the study area (Fig. 1) comprise hydrothermally altered intermediate metavolcanics, metasediments and gabbro, together with intrusive masses of granites and quartz-porphyry. Numerous quartz veins, veinlets, and lenses traverse these rocks. The metavolcanics (basaltic–andesite, andesite, and dacite) consist essentially of plagioclase feldspar, hornblende, quartz, and pyroxenes with minor biotite. Actinolite, zoisite, epidote, chlorite, calcite, apatite, sphene, sericite, biotite, pyrophyllite, alunite, quartz, kaolin, rutile, anatase, pyrite, and magnetite are the alteration products. The metasediments include graphite schist and metamudstone (Oweiss and Khalid 1991). The metasediments are composed mainly of quartz, plagioclase, sericite, chlorite, and epidote. Dissected elongated bodies of fine-grained gabbro occur in the eastern side of Wadi Allaqi (Fig. 1). It is composed of alkali amphiboles, zoisite, saussuritized plagioclase, abundant chlorite, and small grains of rutile. The western coarse-grained gabbros show passage into gabbro–dioritic and granodioritic types. In the rock, quartz and orthoclase appear; however, chlorite, epidote, and hornblende are frequent. The granites are sometimes altered and invaded by pegmatite veins at the southern part. The rock is composed of quartz, orthoclase, amphiboles, and plagioclase partially altered into pyrophyllite and kaolin. The maphic minerals are altered into chlorite, epidote, and zoisite. The quartz-porphyry is almost altered and interfingers with andesites and other rocks. It is composed of quartz, orthoclase, and albite with accessories zircon and apatite. The secondary minerals supported by hydrothermal alterations are pyrophyllite, sericite, quartz, alunite, chalcedony, calcite, kaolin, pyrite, gold, rutile, sphene, albite, chlorite, epidote, magnetite, and hematite (Ivanov 1988).

According to Ramadan et al. (2001), using remote sensing, the Wadi Allaqi area consists of ophiolitic assemblage, island arc assemblage and late- to post-tectonic granitic intrusions. The rocks of ophiolitic assemblage are scattered in the central part and are made up of imbricate thrust sheets and slices of serpentinites, talc carbonate schist, and metagabbros. The island arc assemblage is represented by metasedimentary and metavolcanic-layered units and less abundant intrusive gabbro to diorite plutons. The granitic bodies are widespread in the central part; occur as deeply eroded circular features.

The western part of Wadi Allaqi area was developed through four phases of Neoproterozoic deformations (D_1 through D_4). D_1 is characterized by E-plunging isoclinal folds associated with an E-striking, N-dipping axial planar cleavage. D_2 produced regional thrusts as exemplified by shear zones preserved along Wadi Haimur. Folds are EW striking with W-plunging hinges and steeply N-dipping axial planar cleavage. This phase was associated with remobilized sulfide deposits, and gold-bearing quartz veins. Major WNW–ESE and NW–SE shear zones as well as open folds were formed during D_3, and exposed in the Wadi Allaqi area. Gold bearing quartz veins, wallrock alterations and Cu-sulfide zones were associated with these shear zones. D_4 includes minor E-striking strike-slip faults, intruded by dyke swarms (Kusky and Ramadan 2002).

MATERIALS AND METHODS

Systematic sampling of the drainage pattern has been carried out, 81 stream sediment samples (proluvial and alluvial) were collected for reconnaissance lithochemical survey covering an area of ca 137.59 km^2 with sampling density of ca 1 sample/km^2 (Fig. 1). The samples were taken at ca 50- and 100-m interval, up to a distance of 1.5 km and at a depth of ca 15 cm with about 2-kg weight including high proportion of fresh materials. The selection of size fraction for lithochemical survey in the Eastern Desert of Egypt, characterized by arid climatic condition and predominant mechanical dispersion, was recommended as −1 + 0.25 mm (Bugrov 1974; Bugrov and Shalaby 1975; Arslan 1980; El Bouseily et al. 1985; Darwish and Poellmann 2010). Arslan et al. (1999) found that the −0.25-mm fraction expresses the maximum content of opaque heavy minerals containing sulfides, oxides, and gold grains. However, the −1-mm size fraction was earlier recommended by El-Makky (1982) to be the most appropriate fraction for sampling in the stream sediments and analysis. Accordingly, the raw samples were sieved to obtain −1-mm fraction. In all samples, this fraction was analyzed for S, Cu, Pb, Zn, Mo, Co, Ni, Rb, Ba, Sr, Nb, V, U, Th, Cr, Zr, and Y using pressed powder pellets and a fully automated Philips PW-1404 X-ray fluorescence spectrometer (XRF). The elements La, Ce, and Nd were analyzed using instrumental neutron activation analysis (INAA). These chemical analyses were performed at the Geology Department, Bergen University, Norway. Analysis of Arsenic was conducted also by XRF-technique using "Respect" instrument with energy dispersive spectrometry, Ag-radiation at 35 kV and an anode current of 0.2 mA at the Central Laboratory of Geology University, Moscow. The precision fluctuates from 5 to 10%. The obtained geochemical data were statistically processed via Q-mode cluster and R-mode factor analyses using SPSS (Norusis 1993) and SURFER (Golden-Software, Inc 1994) computer programs.

In order to carry out heavy minerals investigation, ten selected samples near the Au- and Cu-Au mineralizations at Um Garayat area (watershed areas B and C) and the quartz-porphyry stock (watershed area D, Fig. 1), were preliminary treated as mentioned in Carver (1971). These samples were granulometrically analyzed using a set of sieves of 1, 0.5, 0.25, 0.125, 0.0625, and 0.0312 mm. A special focus was done on the −0.25-mm size fraction. It was found that the −0.125 + 0.0625-mm fraction contains the highest heavy minerals residue. The separated opaque and non-opaque heavy minerals, using bromoform heavy liquid, were examined microscopically. Counting was carried out for 300–400 heavy mineral grains in each sample by a point counting method to calculate the opaque/non-opaque ratio and the frequency distribution for non-opaque heavy mineral grain varieties (Table 1).

RESULTS AND DISCUSSION

The Background and Threshold Values

The chemical data were transformed to logarithmic values to testify the statistical distribution of the analyzed elements and are then illustrated as

Table 1. Distribution of the Heavy Minerals in Stream Sediment Samples, Northwestern Part of Wadi Allaqi Area (−0.125 + 0.0625-mm Size Fraction)

Watershed Area	Opaque Minerals	Frequency Percentage (Recalculated to 100%)															
		Opaque	Non-opaque	Non-opaque Minerals													
				Zircon	Tourmaline	Rutile	Hornblende	Pyroxenes	Biotite	Sphene	Garnets	Staurolite	Sillimanite	Epidote	Kyanite	Andalusite	Monazite
Upstream	- Abundant pyrite and arsenopyrite with subordinate pyrrhotite and chalcopyrite.	31.96	68.03	7.38	1.00	1.34	62.75	10.73	5.35	1.34	2.01	1.47	0.00	4.62	0.67	0.00	1.34
		29.16	70.8	5.88	2.00	1.22	54.66	14.70	7.84	1.00	1.96	1.96	0.96	1.94	2.94	0.98	1.96
		43.72	56.27	12.24	1.36	3.40	41.49	16.00	10.55	1.36	2.04	2.04	0.00	4.44	0.00	2.40	3.06
B	- Pyrrhotite is always occurs as fine inclusions in pyrite and arsenopyrite.	47.49	52.50	3.36	1.68	2.94	55.88	17.22	6.30	1.26	1.68	1.26	0.84	3.36	2.10	2.94	0.00
		41.86	58.13	4.00	0.85	2.40	57.60	16.80	4.00	0.85	1.60	1.60	0.00	7.20	0.00	0.00	1.60
Down-stream		41.03	58.96	8.80	4.80	2.40	42.00	17.40	11.00	0.00	4.80	2.40	1.60	4.80	0.00	0.00	0.80
	- Ilmenite.	44.09	55.90	7.45	1.86	1.86	55.29	13.66	7.48	0.00	1.24	1.24	0.00	8.07	0.00	0.00	1.86
	- Titanomagnetite. - Magnetite.																
Upstream C	- Abundant ilmenite with inclusions of pyrite ± pyrrhotite. - Ilmenite is partially or completely decomposed into pseudobrookite, hemoilmenite, sphene and rutile. - Weathering of ilmenite into leucoxene + goethite is commonly observed.	54.26	45.73	3.43	1.96	1.49	51.45	12.25	10.78	0.00	7.36	0.00	0.49	6.37	0.98	0.98	2.45
		36.29	63.73	10.34	2.17	2.00	45.06	14.98	18.46	1.58	3.40	3.34	1.17	0.00	1.58	2.04	3.88
Upstream D	- Titanomagnetite is frequently observed and commonly decomposed into ilmenite and magnetite.	25.76	74.23	10.26	3.30	1.65	48.40	11.57	6.61	3.30	1.65	1.72	2.47	3.95	0.00	1.63	3.47
	- Magnetite contains inclusions of ilmenite ± spinel. - Goethite and lepidocrocite are weathering products of titano-magnetite and magnetite.	Average															
		39.53	60.43	7.31	2.15	2.07	51.45	14.53	7.83	1.06	2.77	1.70	0.75	4.47	0.82	1.09	2.14

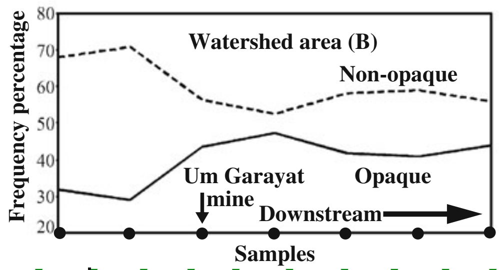

histograms. All elements approximate the lognormal distribution, with different modalities (Table 2). The bimodal elements (As, Cu, S, Pb, Zn, and Ni) and unimodal elements with excess of high values (Mo, Zr, and Ce) could reveal that the studied sediments show evidence of high percentages of anomalous samples allied to mineralization. Whereas, the unimodal elements (Nb, Nd, La, Y, V, Sr, Co, Rb, and U) and those with excess of low values (Ba, Th, and Cr) could characterize the geochemical features of the country rocks within the entire denudation basins. In order to determine the background (C_b) and threshold values (t_1, t_2, and t_3) for each element, Q-mode cluster analysis was applied. The cluster analysis, with the aid of the histograms, differentiates the group of expected background values of each element (for instance As and Cu, Fig. 2). The measures of variability and central tendency of the expected background values were calculated (Table 2), where each element has low variance, almost equal geometric mean, mode and median, with skewness and kurtosis around zero. This reveals that the separated group of expected background values for each element has lognormal distribution and unimodal. Consistent with Lepeltier (1969), the group of expected

Table 2. Determination of Background and Threshold Values of the Analyzed Elements in the Stream Sediments, Northwestern Part of Wadi Allaqi Area

Element	Range (ppm) (n = 81)	Var.	Modality (Data Distribution Form)	Measures of Variability and Central Tendency of the Expected Background Samples									Threshold Values (ppm)			Number and Percent of Anomalous Samples		
				n	Range (ppm)	GSD	Var.	GM (C_b)	Mode	Median	Skewness	Kurtosis	$t_1 = C_b(GSD)$	$t_2 = C_b(GSD)^2$	$t_3 = C_b(GSD)^3$	t_1	t_2	t_3
As	1.5–296	1.888	Bimodal	26	1.5–3	1.31	1.03	1.79	1.50	1.50	1.12	−0.44	2.35	3.07	4.02	61–75.3	55–67.9	52–64.2
Cu	17–2912	1.426		56	17–50	1.31	1.03	32.43	29.99	32.51	−0.28	−0.56	42.48	55.65	72.91	34–41.9	25–30.9	22–27.2
S	340–2900	1.089		56	340–610	1.20	1.01	457.09	349.95	460.26	−0.07	−1.28	546.68	653.83	781.98	38–46.9	22–27.2	12–14.8
Pb	7–66	1.191		34	7–20	1.35	1.04	11.97	14.99	11.48	0.19	−0.83	16.16	21.82	29.45	52–64.2	47–58.0	39–48.1
Zn	33–88	1.023		45	33–55	1.13	1.01	45.49	39.99	46.03	−0.59	−0.32	51.4	58.09	65.64	43–53.1	34–41.9	13–16.1
Ni	19–66	1.033		50	19–35	1.16	1.01	27.04	26.00	26.98	−0.12	−0.49	31.37	36.39	42.21	39–48.2	31–38.3	16–19.8
Nb	4–18	1.052	Unimodal	81	4–18	1.41	1.05	8.51	5.99	8.99	−0.31	−0.58	11.99	16.92	23.86	15–18.5	1–1.2	–
Nd	13–33	1.016		77	13–26	1.19	1.01	20.05	19.01	19.99	−0.45	−0.35	23.86	28.39	33.79	20–24.7	2–2.5	–
La	6–35	1.030		75	11–25	1.22	1.02	14.93	13.00	14.99	0.39	−0.47	18.21	22.22	27.11	11–13.6	4–4.9	1–1.2
Y	15–42	1.016		80	15–34	1.19	1.01	23.28	20.99	23.49	−0.42	−0.01	27.70	32.97	39.23	14–17.3	2–2.5	1–1.2
V	69–200	1.021		81	69–200	1.25	1.02	116.95	100	115.88	0.12	−0.35	146.19	182.73	228.42	16–19.8	2–2.5	–
Sr	100–238	1.019		81	100–238	1.23	1.02	167.49	116.95	179.89	−1.02	−0.05	206.01	253.39	311.68	6–7.4	–	–
Co	6–45	1.059		78	6–30	1.36	1.04	14.76	14.99	14.99	−0.15	0.41	20.07	27.3	37.13	12–14.8	5–6.2	3–3.7
Rb	18–43	1.012		81	18–43	1.18	1.12	28.05	25.00	27.99	0.14	0.20	33.1	39.06	46.09	10–12.4	3–3.7	–
U	1.5–8	1.081		81	1.5–8	1.52	1.08	2.11	1.50	1.50	0.73	−1.01	3.21	4.88	7.41	13–16.1	5–6.2	4–4.9
Mo	1–10	1.300	Unimodal	48	1–2	1.29	1.03	1.12	1.00	1.00	1.80	1.50	1.45	1.86	2.40	41–50.6	41–50.6	33–40.7
Zr	151–687	1.067	(excess of	72	151–459	1.30	1.03	267.92	250.03	267.3	−0.16	−0.38	348.29	452.78	588.62	24–29.6	10–12.4	5–6.2
Ce	24–73	1.023	high values)	59	24–44	1.15	1.01	35.65	34.99	35.98	−0.76	0.21	40.99	47.15	54.22	29–35.8	19–23.5	10–12.4
Ba	157–349	1.009	Unimodal	79	202–349	1.14	1.01	276.69	299.92	279.89	−0.28	−0.45	315.43	359.59	409.93	13–16.1	–	–
Th	2.5–17	1.052	(excess of	81	2.5–17	1.41	1.05	7.60	7.99	7.99	−0.96	1.98	10.72	15.11	21.3	9–11.1	1–1.2	–
Cr	3–167	1.104	low values)	79	62–167	1.25	1.02	110.66	95.06	114.02	−0.20	−0.55	138.33	172.91	216.13	12–14.8	–	–

n number of samples, *GSD* geometric standard deviation, *Var.* variance, *GM* geometric mean, C_b background value.

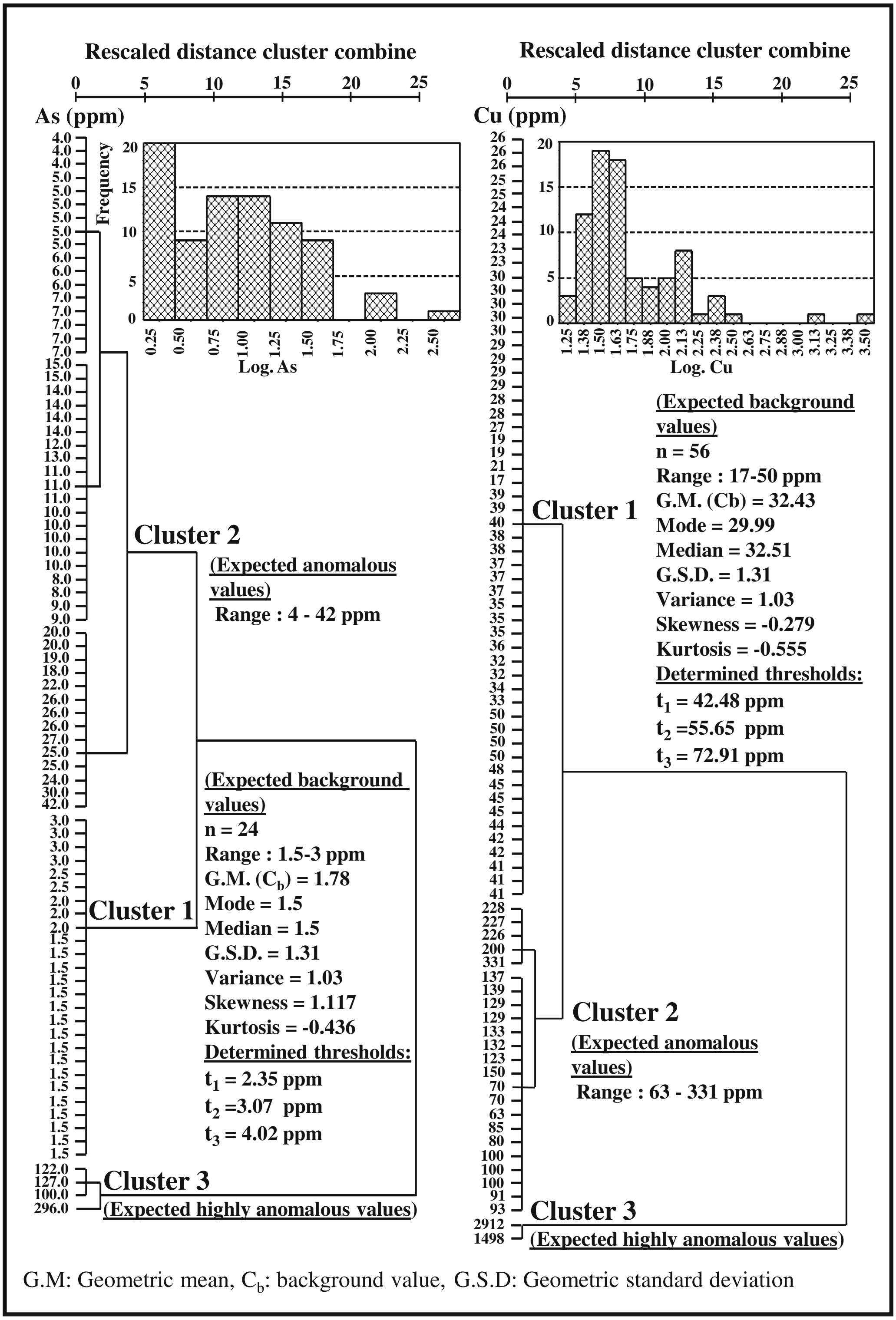

Figure 2. Dendrograms of Q-mode cluster analysis using As and Cu with their histograms for the stream sediment samples (n = 81), northwestern part of Wadi Allaqi area.

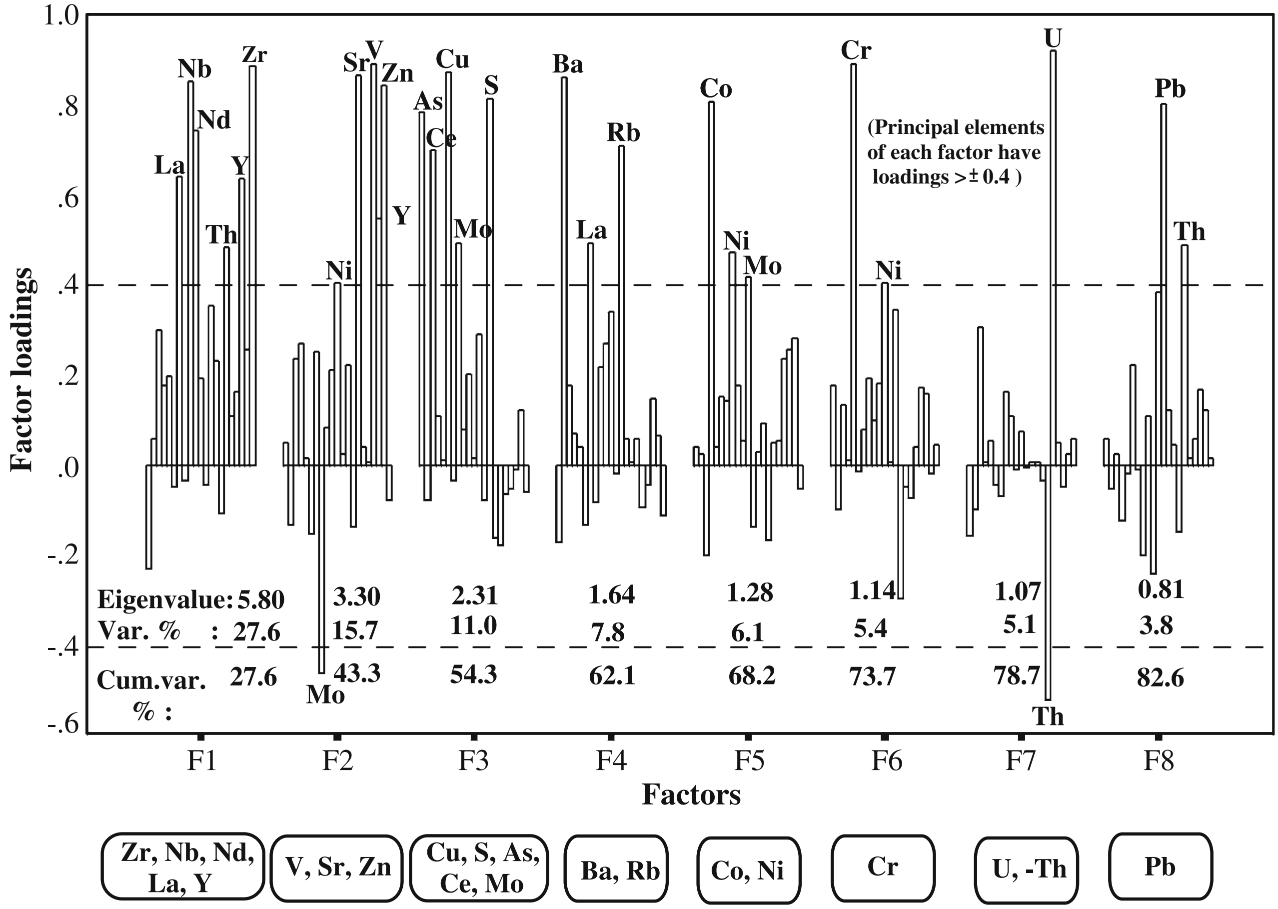

Figure 3. R-mode varimax rotated factor analysis, northwestern part of Wadi Allaqi area.

background values of each element was used to determine the background (C_b = GM, geometric mean) and threshold values: $t_1 = C_b(\mathrm{GSD})$, $t_2 = C_b(\mathrm{GSD})^2$, and $t_3 = C_b(\mathrm{GSD})^3$, where GSD is the geometric standard deviation. The obtained considerable number of anomalous samples using t_3 particularly for As, Cu, S, Pb, Zn, Ni, Mo, and Ce point to confident anomalies in stream sediments (Table 2).

Factor Analysis and Score Maps

The R-mode factor analysis (Fig. 3) examines the relationship between elements in an array of complex data, explaining the original data variability and collecting the elements which appear to behave similarly into groups termed ''factors'' (Tripathi 1979). Factor analysis could show geochemical associations caused by certain geochemical process such as secondary dispersion, mineralization, and alteration. A score on each sample can represent each factor. The score exhibit the effect of the sample and its sharing to create certain factor. Therefore, the factor score map could aid in grouping of samples that are closely related. The significant scores are taken as more than +1 or less than −1.

Factor 1 (Zr, Nb, Nd, La, and Y)

The highest positive scores (Fig. 4) occur in the watershed areas B and D, both drain mainly the metasediments and metavolcanics, in addition to the quartz-porphyry for area D (Fig. 1) and comprise the highest anomalous samples of the associated elements in Factor 1. Zirconium could be due to the primary accessory zircon derived from dacite and quartz porphyry (Ivanov 1988) and characterizing areas B and D with high abundance (Table 1). In addition, Zr tends to admit into apatite replacing

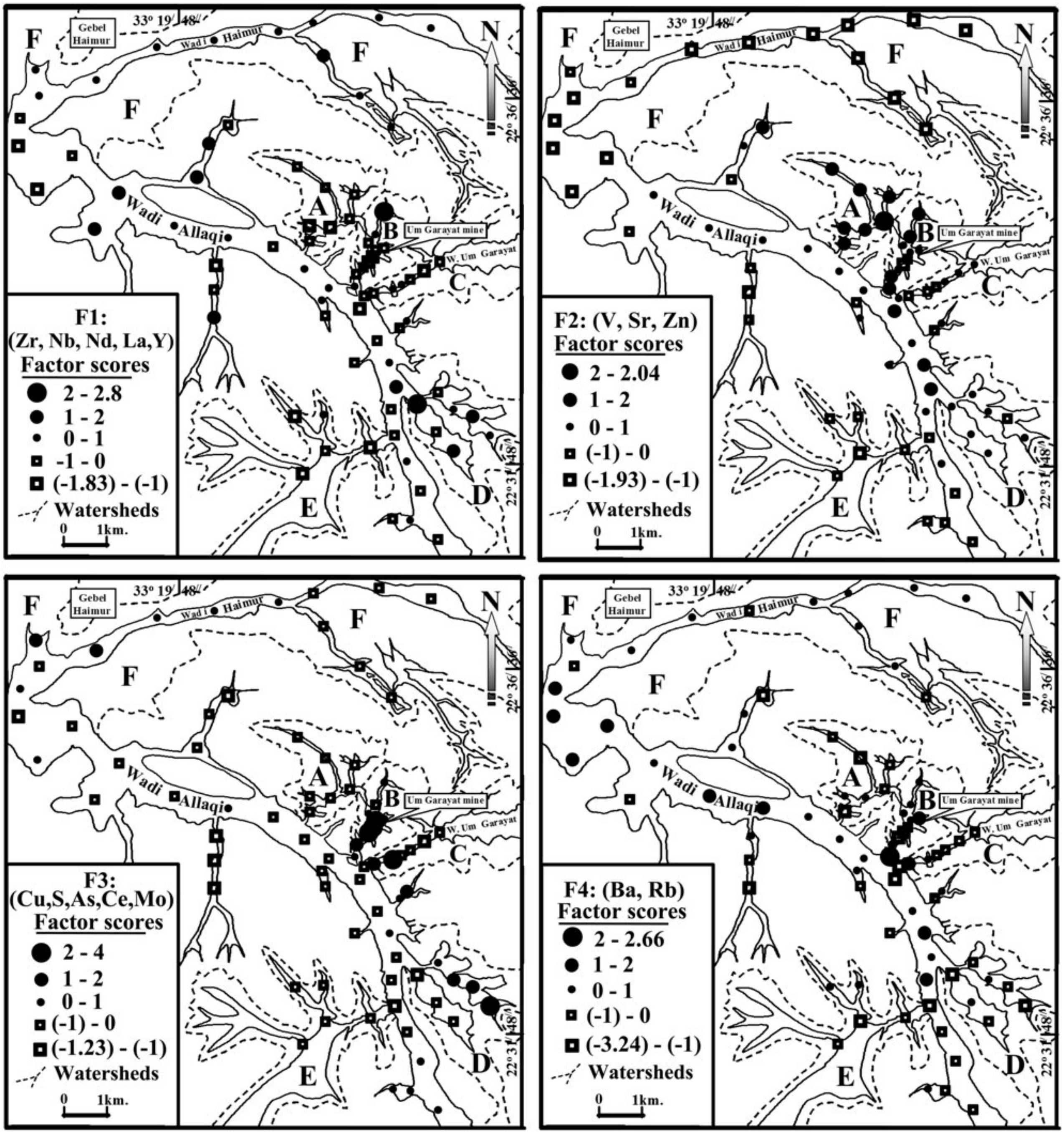

Figure 4. R-mode factor score maps (F1, F2, F3, and F4); northwestern part of Wadi Allaqi area.

Ca (Ringwood 1955), where apatite is present as primary and secondary accessory mineral in the basaltic–andesite and as primary accessory in the quartz porphyry (Ivanov 1988). Niobium substitutes Ti in sphene, rutile, and anatase (Foldvari-Vogl 1978) that exist in the metavolcanics and quartz porphyry as hydrothermal alteration products (Ivanov 1988; El-Nisr 1997). Niobium also could disperse in Ti-bearing minerals particularly biotite (Smirnov et al. 1983), which occurs in dacite and as secondary mineral in the basaltic–andesites and andesites (El-Nisr 1997). Sphene, rutile, and biotite are recorded in areas B and D derived from these rocks (Table 1) as well as zircon that commonly contain Nb and Y (Betekhtin 1961). Niobium also allied to albitization, in zones of hydrothermal alkali metasomatism associating Zr, LREE, and Y (Smirnov et al. 1983), as those developed in the metavolcanics, metasediments, and quartz-porphyry in areas B and D (Ivanov 1988).

In general, Nd, La, and Y could substitute for Ca in primary and secondary Ca-minerals such as apatite as well as calcite and sphene accompanying different types of alterations (Ivanov 1988; El-Nisr 1997) in the metavolcanics at Um Garayat area (B) and the quartz porphyry stock (D). Amphiboles, pyroxenes, zircon, and alunite are also carriers for Nd and La (Szadeczky-Kardoss 1955; Burt 1989; Krauskopf and Bird 1995; Nasraoui et al. 2000). Sphene, amphiboles, pyroxenes, and zircon in addition to garnets that could contain Y (Burt 1989) are recorded in areas B and D (Table 1). Furthermore, Nd and La could be attributed to the zones of alkali metasomatism particularly those accompanying basic rocks (Smirnov et al. 1983) including regional proplytization, carbonitization, sericitization, albitization, and alunitization developed in areas B and D and associating Au-sulfide mineralization (Ivanov 1988). Monazite is recorded in areas B and D (Table 1) that contains Th (subsidiary variable in Factor 1, Fig. 3), La, Nd, and in some instances Y and Zr (Betekhtin 1961; Rose et al. 1979; Burt 1989; Deer et al. 1992). The elements Nd and La could be also ascribed to sediments derived from the zones of supergene kaolinitization formed in these areas (Ivanov 1988), where the LREE could be adsorbed onto kaolinite (Murakami and Ishihara 2008). The associated elements in Factor 1 generally increase also in mudstones (Turekian and Wedepohl 1961; Levinson 1980). Consequently, Factor 1 reveals the sediments drained from the metasediments, metavolcanics, and quartz porphyry and their accompanying zones of alkali metasomatic alterations and supergene kaolinitization associating the Au-sulfide mineralization. The association of Zr, Nb, Nd, La, and Y in Factor 1 could be also due to their immobility in most conditions of the surficial environment (Perelman 1979).

Factor 2 (V, Sr, and Zn)

The highest positive scores (Fig. 4) exist in the watershed areas A and B draining the metasediments, metavolcanics, and gabbro (Fig. 1). Areas A and B include the highest anomalous samples for V, Sr, and particularly Zn. Other positive scores occur in the main stream of Wadi Allaqi close to the watershed area D that has high anomalous samples for Zn, and draining the same above-mentioned rock types as well as the quartz porphyry.

In general, V, Sr, and Zn have the maximum abundance in the mafic minerals of basalts, andesites, and gabbros (Vinogradov 1962; Krauskopf and Bird 1995). These elements could substitute for major cations in silicate structures; Sr^{2+} for Ca^{2+}, V^{3+} for Fe^{3+}, and Zn^{2+} for Fe^{2+}. The wadi sediments in area B contain Ca- and Fe-non-opaque minerals, in addition to ilmenite and magnetite (Table 1). In both latter minerals, the same replacements may occur, including the partial substitution of V^{3+} for Fe^{3+}, while in magnetite Zn^{2+} substitutes for Fe^{2+} (Deer et al. 1992). Moreover, chalcophile elements, such as Zn, are commonly recorded in igneous rocks as tiny sulfide grains. Zinc also associate other chalcophile elements in base metal and precious deposits (Rose et al. 1979) as those of Au-sulfide mineralization in areas B and D, and may be used as pathfinder due to its mobility in surficial oxidizing conditions (Perelman 1979), whereas Sr could be attributed to the zones of carbonatization accompanying this mineralization. Moreover, V, Sr, and Zn increase in mudstones (Turekian and Wedepohl 1961; Levinson 1980). Consequently, Factor 2 could be ascribed mainly to the sediments derived from the metasediments, metavolcanics, gabbro, quartz porphyry, and the zones of carbonatization.

Factor 3 (Cu, S, As, Ce, and Mo)

The highest positive scores (Fig. 4) exist in the watershed areas B, C, D, and F. These areas include the anomalous samples for the associated elements in this factor, with the maximum values in areas B and D. At Um Garayat area (areas B and C), quartz porphyry stock (area D), and Haimur area (F), hydrothermal alteration zones were developed with Au-sulfide mineralization (Ivanov 1988; Darwish 2004). In area B, the stream sediments comprise abundant opaques; pyrite, arsenopyrite, pyrrhotite, chalcopyrite, ilmenite, titanomagnetite, and magnetite with increased frequency percentage in the upper and middle parts of the drainage relative to the mineralization. Areas C and D include abundant ilmenite with inclusions of pyrite and pyrrhotite, titanomagnetite and magnetite (Table 1).

Copper and S of Factor 3 are normally attributed to the sulfides especially those of Cu derived from Um

Garayat (areas B and C, Table 1), quartz-porphyry stock (area D), and Haimur area (F), hosting Au-sulfide mineralizations. Most of arsenic is regarded to arsenopyrite (area B Table 1). It is also found as traces and minor quantities in all the common sulfides including pyrite, substituting for S, and proustite as principal carriers, as well as pyrrhotite, chalcopyrite, sphalerite, galena, and chalcocite, in addition to magnetite and ilmenite and a great variety of secondary oxidation products (Boyle and Jonasson 1973). These minerals exist in the Au-sulfide mineralizations of areas B, C, D, and F (Ivanov 1988; Darwish 2004) and some of them were derived into their stream sediments. Moreover, there is a marked coherence between arsenic and all types of gold deposits, and may accompany Cu in most types of its deposits, serving as a valuable indicator for these metals (Boyle and Jonasson 1973).

Molybdenum could be attributed to magnetite and sphene, which are alteration products in the metavolcanics and quartz porphyry hosting Au-sulfide mineralization, as well as ilmenite, and zircon derived into the stream sediments of areas B, C, and D (Table 1). These accessories are concentrators for Mo (Beus and Grigorian 1977). Furthermore, at Um Garayat area the mineralogical study of panned samples revealed that the wadi sediments contain grains of wulfenite (Oweiss and Khalid 1991), usually found in the zones of oxidation of galena (Foldvari-Vogl 1978). In areas B, C, D, and F, Mo could be especially abundant also in the sulfides of iron and copper as well as galena and sphalerite (Foldvari-Vogl 1978). Accordingly, in the watershed areas B, D, C, and F, the elements Cu, S, As, and Mo could be evidently attributed to the derived sulfide minerals accompanying Au-mineralizations. Moreover, these elements may link also to the ferruginous fragments, mainly limonite, derived as products of sulfides alteration.

Cerium could be ascribed to the weathered materials derived from zones of alkali metasomatic alterations, where LREE could be enriched (Smirnov et al. 1983). These alterations envelop the Au-sulfide mineralizations in areas B, C, D, and F (Ivanov 1988; Darwish 2004). Moreover, Ce substitutes for Ca in the secondary accessory Ca-bearing minerals, accompanying these alterations such as calcite, apatite, sphene, and epidote (Smirnov et al. 1983; Burt 1989). Monazite and zircon also contain some LREE, chiefly Ce as well as some epidote varieties such as allanite (Burt 1989). High abundance of Ce-bearing minerals, monazite, and zircon occur in the stream sediments of areas B, C, and D, in addition to sphene and epidote (Table 1). Cerium could be also adsorbed in zones of supergene kaolinitization (Murakami and Ishihara 2008) associating Au-sulfide mineralization in areas B, C, and D.

Factor 3 undoubtedly defined as the mineralization factor. Arsenic, Cu, S, and Mo concentrate in the ore minerals and are mobile elements in the secondary environment. In the study area, these elements could be considered as direct indicators in the stream sediments survey for the Au-sulfide mineralizations, while Ce associate the alkali metasomatic alteration zones and may be considered as indirect indicator partially migrates in oxidizing conditions (Perelman 1979).

Routhier (1963), Boyle (1979), and Lanckneus (1989) referred to the relation between the gold concentration and the heavy minerals distribution of the stream sediments. The highest concentration of gold grains occurs in the upstream parts intensively associated with ultrastable grains of zircon, tourmaline, and rutile (ZTR), especially zircon. In the downstream parts, the heavy minerals show richness of the metastable heavy mineral grains such as epidote, andalusite, and sphene. Zircon, rutile, and monazite are markedly increases upstream in the watershed area B and somewhat in areas C and D, whereas epidote increase downstream particularly in area B (Table 1). This is considered as a sign for the presence of gold grains derived from the Au-mineralization at Um Garayat (areas B and C) and the quartz-porphyry stock (area D). This is supported by the existence of pronounced arsenic anomalies in these areas, which is the principal indicator of Au and sulfides in the stream sediments geochemical survey (Boyle and Jonasson 1973).

The quartz-porphyry stock hosting Au-sulfide mineralization, at the southeastern part (Fig. 1), consists of different assemblages of granodiorite and quartz-andesite porphyries and represents porphyry copper deposits (Hussein 1990). The watershed area (D) drains the quartz-porphyry and includes Cu–S–As–Mo association with anomalous samples for Pb and Zn. This element association particularly Cu–Mo characterizes the porphyry copper deposits; besides Cu, Mo, and Zn are significant pathfinders for these deposits (Boyle 1974; Foldvari-Vogl 1978; Levinson 1980).

Factor 4 (Ba and Rb)

The maximum positive score occurs nearby the entry of Wadi Um Garayat in the watershed area B

(Fig. 4), which includes anomalies for Ba and Rb, draining small intrusion of granites, as well as metavolcanics, metasediments, and gabbro (Fig. 1). Other positive scores are scattered along the main stream of Wadi Allaqi draining granites of the western part. Barium and Rb exist in basalts, gabbros, and andesites in considerable concentrations, and have the maximum abundance in granites (Vinogradov 1962) as well as in mudstones (Turekian and Wedepohl 1961; Levinson 1980). The cations Ba^{2+} and Rb^{+} tend to substitute for K^{+} and enter potassium minerals (e.g., micas and feldspars), hence are concentrated in acidic rather than basic rocks. However, Ba^{2+} tends to enter early potassium minerals (e.g., biotite, which exist in area B, Table 1), while Rb^{+} is enriched during post-magmatic processes in the K-minerals of the late hydrothermal stage. Barium and Rb can accommodate in the secondary K-minerals such as sericite and alunite developed during the alteration processes (Boyle 1974; Krauskopf and Bird 1995). Accordingly, Factor 4 could be attributed to the weathered materials drained chiefly from the granites all over the explored area, as well as the metasediments and the zones of alunitization and sericitization associating the Au-sulfide mineralization at Um Garayat area (Ivanov 1988), and ascribed somewhat to the metavolcanics and gabbro.

Minor Factors

In Factor 5 (Co and Ni), the highest positive scores (Fig. 5) are located in watershed areas A, B, and D draining the metasediments, metavolcanics, and quartz porphyry (area D), as well as area F draining serpentinites, metagabbros, metasediments, and metavolcanics (Fig. 1). Cobalt and Ni could enrich in the mudstones (Turekian and Wedepohl 1961; Levinson 1980) as well as serpentinites and exist in gabbros, basalts, and andesites in the mafic minerals (Vinogradov 1962; Rose et al. 1979; Krauskopf and Bird 1995). Cobalt is an isomorphous substitute of both Fe and Mg, while Ni substitutes Mg (Foldvari-Vogl 1978) such as in pyroxenes, hornblende, and biotite recorded in the wadi sediments of areas B and D with high percentages (Table 1). Furthermore, Um Garayat area (B) and the quartz porphyry (area D) comprise Au-sulfide mineralization including pyrite, pyrrhotite, chalcopyrite, chalcocite, and covellite (Ivanov 1988) as well as arsenopyrite in the stream sediments (area B, Table 1). At the northwestern part (Gebel Haimur, area F), the sulfide minerals chalcopyrite, arsenian pyrite, sphalerite, and galena associate with the Au-mineralization (Darwish 2004). Cobalt and Ni are associated mainly in Fe-sulfides, particularly arsenian pyrite, and in Cu-ores (Bateman 1952; Reich et al. 2005). Moreover, Co incorporates in sphalerite (Axelsson and Rodushkin 2001). Cobalt and Ni enter the lattices of almost all the mentioned sulfides, and may be used as possible pathfinders (Levinson 1980). The wadi sediments in areas B and D contain also grains of magnetite (Table 1), in which small amounts of Co and Ni can substitute for Fe (Deer et al. 1992). Factor 5 is attributable to the weathering products derived from the metasediments, metavolcanics, serpentinites, and particularly the sulfides associating the Au-mineralizations all-over the survey area.

Factor 6 (Cr) has few positive scores in watershed areas A, B, and F (Fig. 5). These scores could be due to the existence of serpentinites (area F), as well as Cr in the pyroxenes (Vinogradov 1962; Krauskopf and Bird 1995) derived from the metavolcanics (area B, Table 1; Fig. 1). Chromium is present in mudstones (Turekian and Wedepohl 1961; Levinson 1980), where it is introduced in clayey sediments by micas, hydromicas, illites, and chlorites (Foldvari-Vogl 1978), and could be ascribed to the metasediments (Fig. 1). Magnetite grains were also detected in the stream sediments of area B (Table 1) where magnetite may include partial substitution of Cr for Fe^{3+} (Deer et al. 1992).

In Factor 7 (U and -Th), the highest positive scores with some negative ones are located at the southern part (Fig. 5), including the highest anomalies for U, and draining mainly granites, metasediments, and gabbro (Fig. 1). The granites are invaded by pegmatite veins (Ivanov 1988), where U and to some extent Th could be enriched in granitic rocks with the maximum abundances in the pegmatitic and later on in the hydrothermal phase (Foldvari-Vogl 1978). In the study area, the granites are sometimes altered and comprise quartz, orthoclase, amphiboles, plagioclase, epidote, and zoisite. In granites and pegmatites, these minerals could contain U and Th, with high contents in epidote and zoisite (Tauson 1961). Other significant positive and negative scores are located in watershed areas B (including the highest anomalies for Th), C and D draining the metavolcanics, metasediments, gabbro, and quartz-porphyry, as well as in the main stream of Wadi Allaqi draining granites of the western part. In these areas, the wadi sediments include high

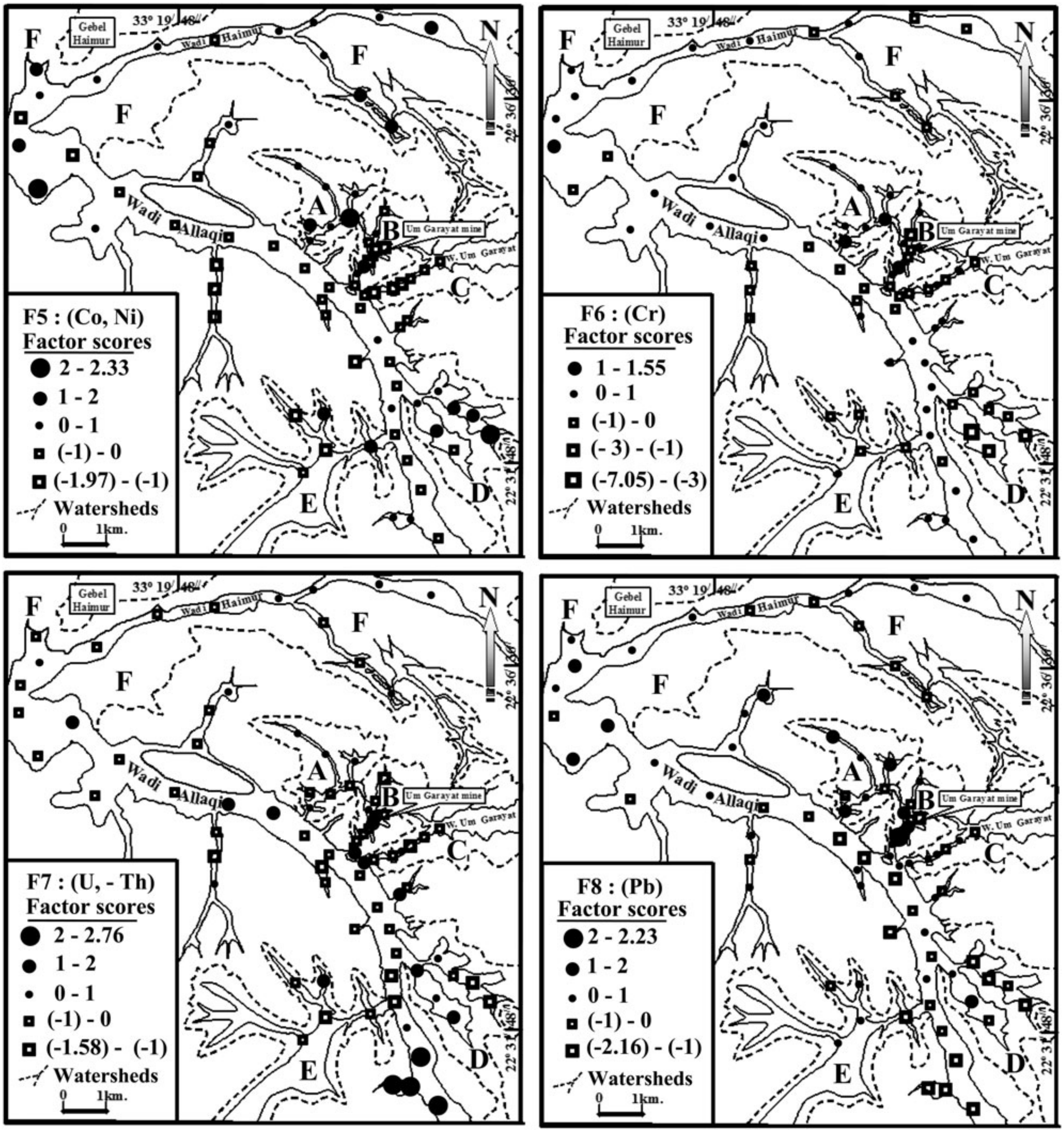

Figure 5. R-mode factor score maps (F5, F6, F7, and F8); northwestern part of Wadi Allaqi area.

abundances of hornblende, pyroxenes, biotite, epidote, zircon, rutile, monazite (2–15% Th), sphene, and ilmenite (Table 1). In these minerals, particularly the resistant accessories such as zircon, monazite, sphene, and apatite, U and Th tend to be highly concentrated (Tauson 1961; Rose et al. 1979; Smirnov et al. 1983). Apatite could be derived from the basaltic–andesite and quartz porphyry (Ivanov 1988). This factor could be attributed to the rock-forming minerals and accessories derived chiefly from the granites and its associated pegmatites at the southern part in addition to those derived from the quartz porphyry, metasediments, metavolcanics, and gabbro.

Factor 8 (Pb) displays a cluster of the highest positive scores in watershed area B (Fig. 5), including the highest anomalies of Pb. This area drains hydrothermally altered intermediate metavolcanics hosting Au-sulfide mineralization, metasediments, and granites (Fig. 1). Chalcopyrite often contains Pb or inclusions of galena, whereas pyrite contains minor contents of Pb (Levinson 1980; Deer et al. 1992). In acidic and intermediate rocks, zircon and magnetite are carriers for Pb (Beus and Grigorian 1977). In area B, all these minerals were recorded in the wadi sediments (Table 1) as well as wulfenite (Oweiss and Khalid 1991), in addition to disseminated galena in some quartz veins (El-Makky 2000). Furthermore, K-minerals are carriers of the majority of Pb in rocks (Beus and Grigorian 1977). Pb^{2+} tends to substitute for K^+ in early K-minerals; hence, it is concentrated in acidic rocks and lesser in intermediate ones (Krauskopf and Bird 1995). Accordingly, in area B, Factor 8 could be ascribed to the sulfides, magnetite, zircon, wulfenite, and K-minerals, derived from the Au-sulfide mineralization, metavolcanics, and granites. Other positive scores and anomalous samples occur in the watershed areas A, D, and F. In area A, the scores could be attributed to the weathered materials derived from the metavolcanics and metasediments, where the mudstones could contain increased contents of Pb (Turekian and Wedepohl 1961; Levinson 1980). In area D, zircon, magnetite, and pyrite were recorded (Table 1) as carriers for Pb in addition to chalcopyrite and orthoclase. These minerals could be derived from the quartz porphyry, hosting Au-sulfide mineralization, as well as the metavolcanics. In the northwestern part near Gebel Haimur (area F), the positive scores could be attributed to the existence of chalcopyrite, pyrite, and galena (Darwish 2004) associating Au-mineralization. In the survey area, Pb as mobile to slightly mobile element in surficial oxidizing conditions (Perelman 1979) may be used as pathfinder for the sulfide minerals.

Enrichment Factor

Factor score maps that display geochemically related group of samples may hide some valuable anomalous values for individual elements. Therefore, in the mineralization Factor 3 (Cu, S, As, Ce, and Mo), the enrichment factor was determined for each element. The enrichment factor (EF_j^i) is a convenient way to compare a given sample to a chosen reference material. It is defined as the concentration ratio of a given element i and the normalizing element j (X_i/X_j), in the given sample divided by the same ratio in the reference material (average in upper continental crustal rocks), i.e., $EF_j^i = (X_i/X_{j,\text{sample}})/(X_i/X_{j,\text{reference}})$. An EF_j^i value of >1 represents enrichment of element i in the sample as compared to the reference, whereas a value <1 means depletion (Li 2000).

In order to select the appropriate normalizing element, the determined variances for the analyzed elements (Table 2) are illustrated in Figure 6a. It is clear that Rb and Ba have the lowest variances reflecting that each element has low variability and approximately constant values in the samples. Moreover, the few anomalous values for these elements, particularly Rb (Table 2), are not coincided with the anomalies of As, Cu, and S (Fig. 6b, c) that have the highest loadings in the mineralization Factor 3 (Fig. 3). In addition, Ba and Rb are associated together in Factor 4 and are slightly mobile in the surface condition (Perelman 1979; Rose et al. 1979). The enrichment factors were determined in each sample for As, Cu, and S using Rb and then Ba as normalizing elements as well as for Mo and Ce using Rb (Fig. 7). It is observable that the obtained values of the enrichment factors using Rb are higher than those with Ba particularly for As, Cu, and S. Therefore, the enrichment factors were determined for the anomalous samples (at t_1) of the elements associated in the mineralization factor using Rb as the normalizing element to exhibit the enrichment sites for each element. The average abundances of As, Cu, S, Mo, Ce, and the normalizing element Rb in the continental crust are based on Krauskopf and Bird (1995).

In addition, the contrast index (CI) was calculated for the obtained EF values for each element (Table 3) as $CI = EF_{max}/mean_{low\ values}$ (Beus and Grigorian 1977; Rose et al. 1979). The low values of EF for each element were selected using sorting curve. In the present case, the contrast of enrichment expresses its strength as a ratio to the average of low values. The resulted contrast indexes reveal that $As > Cu > Mo > S > Ce$, reflecting that As and Cu have the maximum enrichment in the survey area.

According to the distribution of enrichment factors for the anomalous samples (Fig. 8a) within each watershed area, generally, Cu, S, As, Ce, and Mo are highly enriched in the upper and middle parts along the drainages relative to the mineralized sites, particularly in areas B, C, and D. The enrichment gradually decreases in the down stream direction. This enrichment reflects short dispersion

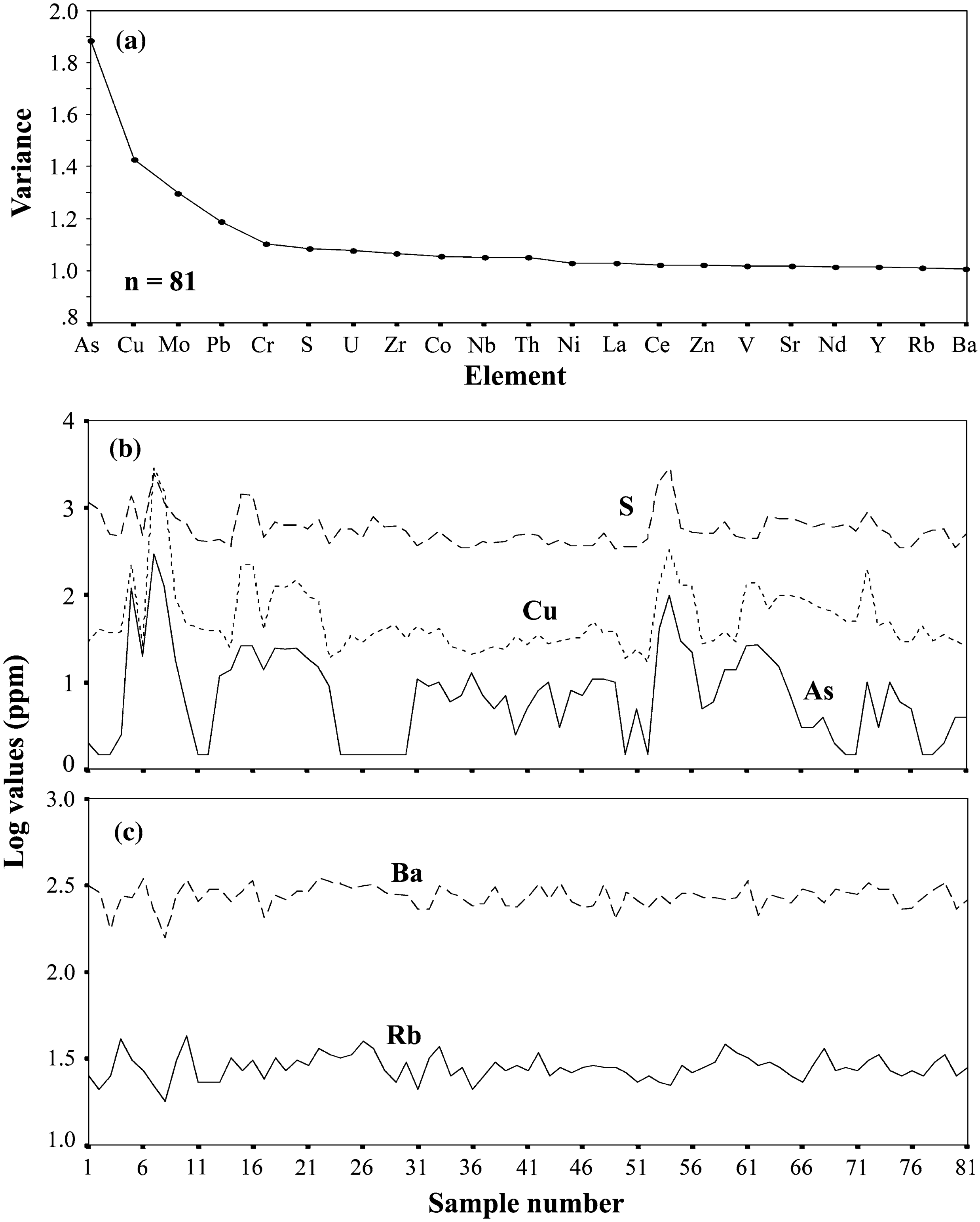

Figure 6. **a** Variance of the analyzed elements; **b**, **c** contents of As, Cu, S, Rb, and Ba in the stream sediment samples, northwestern part of Wadi Allaqi area.

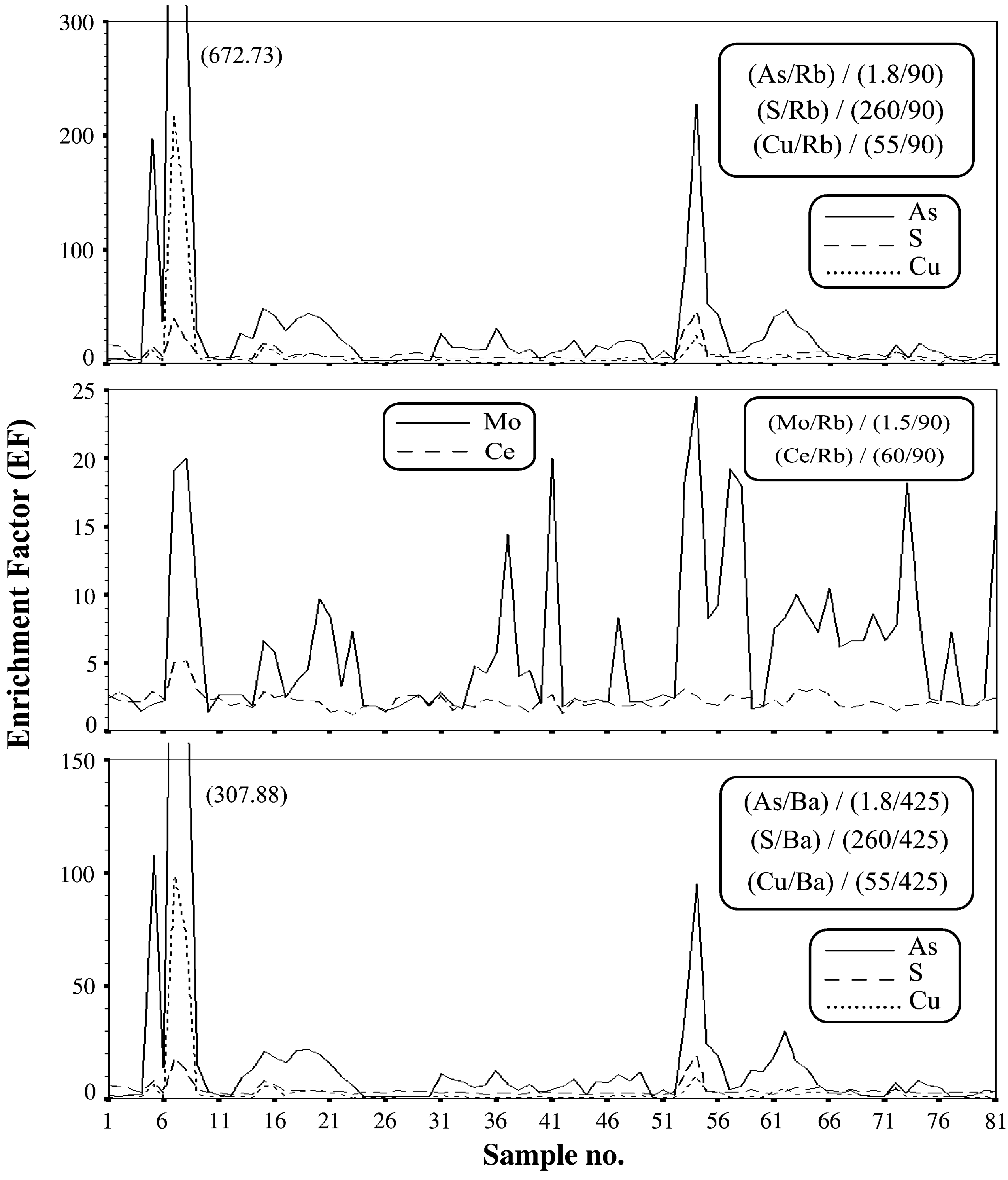

Figure 7. Enrichment factors for As, S, Cu, Mo, and Ce; northwestern part of Wadi Allaqi area.

trains (ca 1 km) mainly controlled by the prevailed mechanical state of migration for the minerals hosting these elements in that arid region. However, the seasonal torrents could aid in transporting mechanical disintegration products for longer distances downstream. The variations in force of water

Table 3. Determination of the Contrast Indices for the Enrichment Factors of As, Cu, S, Mo, and Ce in the Stream Sediment Samples, Northwestern Part of Wadi Allaqi Area

Element	Low Values of EF	Statistical Parameters for the Low Values of EF					Contrast Index (CI) = $EF_{max}/mean_{low\ values}$
		n	Mean	SD	Var.	Range	
As	(As/Rb)/(1.8/90) < 25	58	8.98	6.21	38.56	1.88–21.88	672.8/8.98 = 74.92
Cu	(Cu/Rb)/(55/90) < 10	74	2.99	2.07	4.28	0.94–9.46	216/2.99 = 72.48
Mo	(Mo/Rb)/(1.5/90) < 3	40	2.14	0.38	0.15	1.4–2.86	24.55/2.14 = 11.47
S	(S/Rb)/(260/90) < 8	63	5.85	1.04	1.07	3.89–7.82	45.64/5.85 = 7.8
Ce	(Ce/Rb)/(60/90) < 2	33	1.73	0.22	0.05	1.18–1.99	5.17/1.73 = 2.99

EF enrichment factor, *SD* standard deviation, *Var.* variance.

flow along the drainages make favorable conditions for mechanical barriers, where the velocity of water may sharply decrease due to bends and obstructions. Therefore, the hosting opaque heavy minerals, particularly the abundant sulfides and oxides (Table 1; Fig. 8b), generally accumulate in the fine fraction (−0.125 + 0.0625 mm) as proluvial sediments. Proportions of the products could pour into the alluvial sediments indicated by the occurrence of some anomalous samples for these elements in the main stream of Wadi Allaqi (Fig. 8a).

In the stream sediments draining the Au-sulfide mineralization of Um Garayat area (areas B and C), the presence of malachite, azurite, and wulfenite (Oweiss and Khalid 1991; Abdel Rahman et al. 2001) that usually form in the oxidation zones of mineralization as well as widespread limonite (Ivanov 1988) reflect products and a certain period of chemical weathering processes. The surface and ground water may cause supergene chemical destruction of the mineralization as well as its primary and secondary halos. The seasonal torrents play also a minor role in the hydromorphic dispersion of the concerned elements. In aqueous migration, these elements have different mobilities (S > Cu, Mo > As) in oxidizing conditions, while, Ce is immobile in most conditions (Perelman 1979). The highly mobile sulfur, which has distinct anomalous samples with low enrichment factors all along the main stream of Wadi Allaqi, could signify the hydromorphic dispersion. This indicates long dispersion trains for S and the occurrence of sulfides source at considerable distances. The torrents led also to simultaneous gradual dilution for the enrichment of these elements in the downstream direction.

Potential Mineralization Sites

The enrichment factor maps (Fig. 8a) verify the interpretation of the mineralization Factor 3 and show that As, Cu, S, Mo, and somewhat Ce are markedly enriched in the stream sediments draining mainly the metavolcanics of Um Garayat area (watershed areas B and C), the quartz-porphyry stock (area D), and Gebel Haimur area (F) hosting Au-sulfide mineralizations.

The watershed areas (A and E) include negative scores for the mineralization Factor 3 (Fig. 4), however, arsenic enriches within these areas (Fig. 8a). Arsenic is relatively mobile in primary mineralization processes. In shear zones, such as Allaqi containing arsenic-bearing deposits, arsenic could find its way into many subsidiary fractures, migrates far in advance of the main wave of mineralization. Consequently, the primary arsenic halos and the dispersion terrains developed on their upward extensions could be broad. In stream sediment surveys, arsenic is a particular indicator for gold deposits in various terrains and under a variety of climatic conditions (Boyle and Jonasson 1973). In area (A), the stream sediments drain several quartz veins extending discontinuously at the surface in the meta-andesites and trending NNE–SSW (El-Makky 2001). This area represents a probable northwest extension of Um Garayat Au-sulfide mineralization. This extension is concordant with the general trends of NW–SE to NNE–SSW for the system of quartz veins and their associated alteration zones (Kochin and Bassyouni 1968; Sabet et al. 1983; Ivanov 1988). Arsenic most probably dispersed mechanically by its carrier heavy minerals. Moreover, under conditions of oxidation, more arsenic may be removed from the oxidizing parts of the ore bodies and ultimately dispersed in surface water. In the stream sediments of area (A), arsenic could precipitate by adsorption on mineral particles, clays and gels, or co-precipitated with all types of hydrous iron oxides and manganese oxides (Boyle and Jonasson 1973). Area (A) includes also enriched and coincided samples for Cu and Mo with background values of S. This may reflect that the weathering products

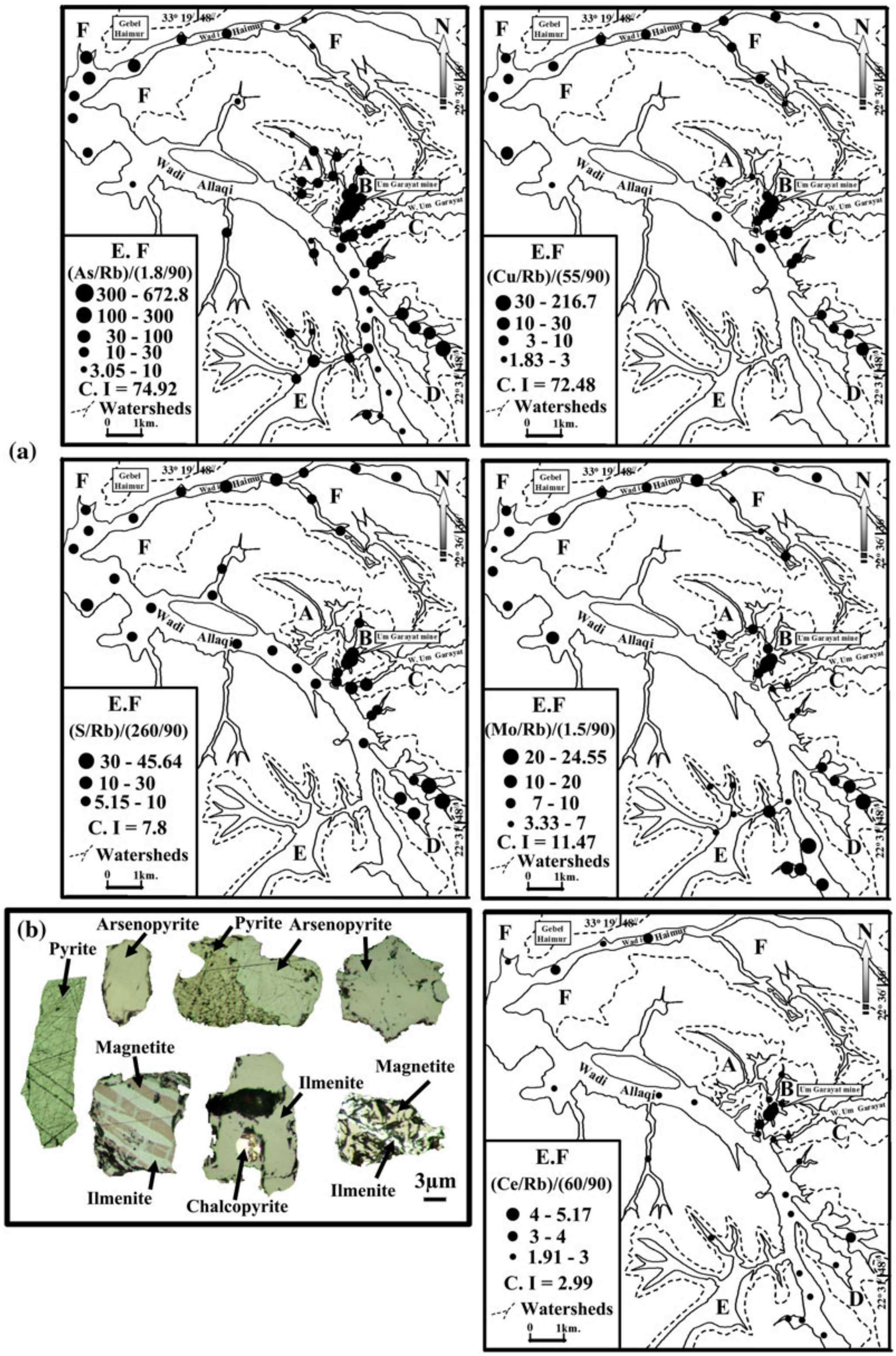

Figure 8. **a** Enrichment factors (EF) for the anomalous samples (at t_1) of As, Cu, S, Mo, and Ce, northwestern part of Wadi Allaqi area, (CI: Contrast Index), **b** Opaque heavy minerals in the stream sediments of watershed areas B, C, and D.

were derived from the oxidation zone of mineralization usually contains secondary Cu-oxides, -carbonates, and -molybdates, while Cu-sulfides were leached down below the oxidation zone. Molybdenum could be also attributed to its concentrator, magnetite (Beus and Grigorian 1977) derived from the metavolcanics. In area (E), the enrichment of arsenic especially in the first- and second-order drainages could reflect some Au-mineralization, where arsenic anomalies usually enrich near the source of the mineralization (Boyle and Jonasson 1973). Areas A and E, possibly signify unexplored extension of Au-sulfide mineralization connected to the main source hosted within the Allaqi shear-zone.

In the extreme southern streams, draining mainly granites traversed by pegmatite veins (Ivanov 1988), Mo is highly enriched in four samples that are also slightly enriched in Ce (Fig. 8a), anomalous for Zr and have both the maximum anomalous contents of U (8 ppm) and positive scores (Fig. 5) for Factor 7 (U and -Th). These maximum contents of U are more than the U content in normal soil (1 ppm) and granite (4.8 ppm, Levinson 1980). In the entire drainages, the U/Th ratios range from 0.09 to 3.2 (maximum in the concerned four samples) with an average value of 0.41. In the pegmatitic phase, the U/Th ratio is usually about 0.2 and increases in the hydrothermal phases due to the decrease of Th content. The association of U with high contents of Mo is typically common in pegmatites that usually enrich in these elements as well as Zr and REE (Boyle and Jonasson 1973; Boyle 1974; Foldvari-Vogl 1978). In these stream sediments, the association of U and Mo with the high U/Th ratio is most probably attributed to the pegmatite veins, which are considered as the available source of U as well as the rock-forming minerals and accessories of granites. Uranium and Mo have variable valences, are strong active migrants in the oxidizing environment (Perelman 1975, 1979; Smirnov et al. 1983), and may be transported in the soluble hexavalent state.

CONCLUSIONS

(1) In the explored area, the highest heavy minerals residue was concentrated in the −0.125 + 0.0625-mm size fraction.

(2) Factors 1 (Zr, Nb, Nd, La, and Y) and 2 (V, Sr, and Zn) are lithological factors, reveal the sediments derived from the metasediments, metavolcanics, quartz-porphyry, and gabbro, and their associated alkali metasomatic alteration zones and supergene kaolinitization enveloping the Au-sulfide mineralization at Um Garayat area and the quartz-porphyry stock.

(3) Factor 3 (Cu, S, As, Ce, and Mo) is the mineralization factor allover the study area. Arsenic, Cu, S, and Mo concentrate in the ore minerals, and are considered as direct indicators in the stream sediments survey for the Au-sulfide mineralizations, while Ce incorporates in the secondary accessory Ca-bearing minerals accompanying the alkali metasomatic alterations enveloping the mineralization and may be an indirect indicator. The Cu–S–As–Mo association with Pb and Zn anomalies in the watershed area draining the quartz-porphyry stock reflects its porphyry copper mineralization.

(4) Factor 4 (Ba and Rb) is connected to the weathered materials drained chiefly from the granites all over the explored area, as well as the zones of alunitization and sericitization associating the Au-sulfide mineralization at Um Garayat area.

(5) In the entire stream sediments of the survey area, Co and Ni are pathfinders for the Fe- and Cu-sulfides, associating Au-mineralizations, while Zn and Pb are probable supplementary pathfinders for the Au-sulfide mineralizations.

(6) The southern part comprises granites and pegmatite veins with high U/Th ratios and U–Mo association in its drained stream sediments. In the wadi sediments draining Um Garayat area and the quartz-porphyry stock, high abundances of hornblende, pyroxenes, biotite, and particularly the accessories monazite, zircon, epidote, sphene, and ilmenite were accumulated. These parts could represent available sources of U and Th in the explored area.

(7) The contrast indices for enrichment factors reveal that As and Cu have the maximum enrichment in the survey area. Two unexplored areas contain marked enrichment for arsenic and could represent the extension of Au-sulfide mineralization linked to its source of the Allaqi shear-zone.

(8) The enrichment of the mineralization Factor 3 (Cu, S, As, Ce, and Mo), somewhat near the mineralized sites could be explained by the dominant processes of mechanical disintegration with minor sharing of chemical weathering. Subsequently, the products were transported mechanically with the aid of seasonal torrents that also caused minor hydromorphic dispersion as well as gradual downstream dilution for the elements of Factor 3.
(9) From an exploration point of view, the R-mode factor analysis reduced many variables into eight factors and provided easily and reasonably interpretable results. The enrichment factors for the associated elements in the mineralization factor produced vital results during the stream sediments survey indicative of a promising area for detailed exploration.

ACKNOWLEDGMENTS

The authors thank two anonymous Journal reviewers and Chief Editor Prof. K. R. Long for their constructive comments and time spent revising and improving this manuscript. We sincerely appreciate Prof. M. M. El-Sayed Dean of the Faculty of Science, Damanhour University, Egypt for performing the chemical analyses at the Geology Department, Bergen University, Norway, as well as Prof. V. Goorvitch Chief of the Central Laboratory of Geology University, Moscow.

REFERENCES

Abdel Rahman, E., Fawzy, K. H. M., & El-Mohammady, S. (2001). Geochemical studies on placer gold deposits at Um Grayat gold mine, south Eastern Desert, Egypt. In *5th conf. geochem*. (Vol. 2, pp. 395–403), Geological Department, Alexandria University.

Afia, M. S., & Imam, I. (1979). *Mineral map of Egypt, scale 1: 2000,000, with explanatory notes and lists*. Geological Survey of Egypt.

Anwar, Y. M., Morsy, M. A., Arslan, A. I., & El Makky, A. M. (1984). Estimation of the probable geological reserve of tin in Igla area, Eastern Desert of Egypt. In *Abstracts of the 3rd symposium on Precambrian and development* (p. 5), NIDC, Cairo.

Arslan, A. I. (1980). Methods of lithochemical prospecting for gold deposits in the Eastern Desert of Egypt, Ph. D. Thesis, Moscow State University.

Arslan, A. I., Khalil, S. O., Mohamed, F. H., & El Deeb, H. M. (1999). Prospective geochemical and heavy mineral surveys around El Eradiya gold mine central Eastern Desert, Egypt. In *The 1st international conference on the geology of Africa* (Vol. I, pp. 391–402), Assiut, Egypt.

Axelsson, M. D., & Rodushkin, I. (2001). Determination of major and trace elements in sphalerite using laser ablation double focusing sector field ICP-MS. *Journal of Geochemical Exploration, 72*(2), 81–89.

Bateman, A. M. (1952). *Economic mineral deposits* (2nd ed.). New York: Wiley.

Betekhtin, A. G. (1961). *A course of mineralogy*. Moscow: Peace Publishers.

Beus, A. A., & Grigorian, S. V. (1977). *Geochemical exploration methods for mineral deposits*. Wilmette, IL: Applied Publishing.

Boyle, R. W. (1974). Elemental associations in mineral deposits and indicator elements of interest in geochemical prospecting. *Geological Survey of Canada*, Paper 74-75.

Boyle, R. W. (1979). The geochemistry of gold and its deposits. *Geological Survey Canada Bulletin, 280*.

Boyle, R. W., & Jonasson, I. R. (1973). The geochemistry of arsenic and its use as an indicator element in geochemical prospecting. *Journal of Geochemical Exploration, 2*, 251–296.

Bugrov, V. A. (1974). Geochemical sampling techniques in the Eastern Desert of Egypt. *Journal of Geochemical Exploration, 3*, 67–75.

Bugrov, V. A., & Shalaby, I. M. (1975). Geochemical prospecting in the Eastern Desert of Egypt. In *Proceedings of the 5th international geochemical exploration symposium*, Vancouver, 1974, Elsevier.

Burt, D. M. (1989). Compositional and phases relations among rare earth element minerals. In B. R. Lipin & G. A. McKay (Eds.), *Geochemistry and mineralogy of rare earth elements* (Vol. 21, pp. 259–307). Reviews in Mineralogy. Washington, DC: Mineralogical Society of America.

Carver, R. E. (1971). *Procedures in sedimentary petrology*. New York: Wiley.

Darwish, M. A. G. (2004). Geochemical exploration for the gold in Haimur area, Wadi Allaqi, south eastern Desert, Egypt. Ph. D. Thesis, Aswan, Fac. Sci., South Valley Univ., Egypt.

Darwish, M. A. G., & Poellmann, H. (2010). Geochemical exploration for gold in the Nile Valley Block (A) area, Wadi Allaqi, South Egypt. *Chemie der Erde, 70*, 353–362.

Deer, W. A., Howie, R. A., & Zussman, J. (1992). *An introduction to the rock forming minerals* (2nd ed.). Essex: Longman Scientific & Technical Group Ltd.

El Bouseily, A. M., Arslan, A. I., Ghoneim, M. F., & Harraz, H. Z. (1985). Mercury dispersion patterns around El Sid—Fawakhir gold mine, Eastern Desert, Egypt. *Journal of African Earth Sciences, 5*(5), 465–469.

El Kazzaz, Y. A., & Taylor, W. E. G. (1996). A tectonic-stratigraphy of Neoproterozoic in Wadi Allaqi, south Eastern Desert, Egypt. In *Proceedings of the Egyptian geological survey centennial conference, Cairo* (pp. 225–262).

El Ramly, M. F. (1972). A new geological map for the basement rocks in the Eastern and Southwestern Deserts of Egypt. *Annals of Geological Survey of Egypt, 2*, 1–18.

El-Kazzaz, Y. A. (1995). Tectonics and mineralization of Wadi Allaqi, south Eastern Desert, Egypt. Ph.D. Geol. Luton Univ. London, England.

El-Kazzaz, Y. A. (1996a). Shear zone hosted gold mineralization in south Eastern Desert, Egypt. In *Proceedings of the Egyptian geological survey centennial conference, Cairo* (pp.185–204).

El-Kazzaz, Y. A. (1996b). Speculations on the tectonic evolution of central Wadi Allaqi, south Eastern Desert, Egypt. In *Proceedings of the Egyptian geological survey centennial conference, Cairo* (pp. 205–223).

El-Makky, A. M. (1982). Geochemical prospecting at Mersa Alam area, Eastern desert, Egypt. M.Sc. Thesis, Alexandria University.

El-Makky, A. M. (2000). Applications of geostatistical methods and zonality of primary haloes in geochemical prospecting at the Um Garayat gold mine area, south Eastern Desert, Egypt. *Delta Journal of Science, 24*, 159–192.

El-Makky, A. M. (2001). Trend surface analysis as an exploration guide in the environs of Um Garayat gold mine area, South Eastern Desert, Egypt. In *(Abs.) 2nd international conference on geology of Africa* (Vol. III-21, pp. 38–39), Assiut University.

El-Nisr, S. A. (1997). Late Precambrian volcanism in Wadi El Allaqi area southeastern Desert, Egypt: An evidence for transitional continental arc/margin environment. *Journal of African Earth Sciences, 24*, 301–313.

Foldvari-Vogl, M. (1978). *Theory and practice of regional geochemical exploration*. Budapest: Akademiai Kiado.

Golden-Software, Inc. (1994). *Surfer for windows package*. Golden, CO: Golden Software, Inc.

Hunting Geology and Geophysics Ltd. (1967). *Assessment of the mineral potential of the Aswan region U. A. R., photogeological survey*. United Nation Development Program, United Arab Republic. Regional Planning of Aswan.

Hussein, A. A. (1990). Mineral deposits of Egypt. In R. Said (Ed.), *The geology of Egypt* (pp. 511–566). Rotterdam, Brookfield: A. A. Balkema.

Ivanov, T. G. (1988). Report of study of hydrothermal alterations in localities Um Garayat and Um Tundup, southeastern Desert, Egypt. United Nations Development Programme in the Arab Republic of Egypt. Geol. Surv. Egypt (Internal Report).

Ivanov, T. G. & Hussein, A. A. (1972). Report on geological operations in the assessment of the mineral potential of the Aswan region, Project from July 1968 to June 1972. Aswan Mineral Surv. Project., Geol. Surv. Egypt (Internal Report).

Kochin, G. G., & Bassyouni, F. A. (1968). Mineral resources of the U.A.R., Part I. Metallic minerals. Geol. Surv. Egypt (Internal Report).

Krauskopf, K. B., & Bird, D. K. (1995). *Introduction to geochemistry* (3rd ed.). New York: McGraw-Hill, Inc.

Kusky, T. M., & Ramadan, T. M. (2002). Structural controls on Neoproterozoic mineralization in the South Eastern Desert, Egypt: An integrated field, Landsat TM, and SIR-C/X SAR approach. *Journal of African Earth Science, 35*, 107–121.

Lanckneus, J. (1989). The use of heavy minerals as pathfinders for placer gold. A case study in the department of Madre De Dios (SE PERU). *Bulletin Van de Belgische Vereninging Voov Geologie, 98-91*, 63–72.

Lepeltier, C. (1969). A simplified statistical treatment of geochemical data by graphical representation. *Economic Geology, 64*, 538–550.

Levinson, A. A. (1980). *Introduction to exploration geochemistry* (2nd ed.). Wilmette, IL: Applied Publishing.

Li, Y. H. (2000). *A Compendium of geochemistry: From Solar Nebula to the Human Brain*. Princeton, NJ: Princeton University Press.

Murakami, H., & Ishihara, S. (2008). REE mineralization of weathered crust and clay sediment on granitic rocks in the Sanyo Belt, sw Japan and the southern Jiangxi province, China. *Resource Geology, 58*(4), 373–401.

Nasraoui, M., Toulkeridisb, T., Clauerb, N., & Bilala, E. (2000). Differentiated hydrothermal and meteoric alterations of Lueshe carbonatite complex (Democratic Republic of Congo) identified by a REE study combined with a sequential acid-leaching experiment. *Chemical Geology, 165*(1–2), 109–132.

Norusis, M. J. (1993). *Statistical package for the social sciences (SPSS for Windows)*. Chicago: SPSS Inc.

Obeid, M., Ali, M., & Mohamed, N. (2001). Geochemical exploration on the stream sediments of Gabal El Mueilha area, central Eastern Desert, Egypt: An overview on the rare metals. *Resource Geology, 51*(3), 217–227.

Oweiss, Kh. A., & Khalid, A. M. (1991). Geochemical prospecting at Um Qareiyat gold deposits, South Eastern Desert, Egypt. *Annals. Geological Survey of Egypt, 17*, 145–151.

Perelman, A. I. (1975). *Geochemistry of landscape*. Moscow: High School Pub. (in Russian).

Perelman, A. I. (1979). *Geochemistry*. Moscow: High School Pub. (in Russian).

Ramadan, T. M., Abdelsalam, M. G., & Stern, R. J. (2001). Mapping gold-bearing massive sulfide deposits in the Neoproterozoic Allaqi suture, southeast Egypt with landsat TM and SIR-C/X SAR Images. *Photogrammetric Engineering & Remote Sensing, 67*(4), 491–497.

Rashwan, A. A., Taylor, W. E. G., & El Kazzaz, Y. A. (1995). Geology and structural evolution of Wadi Um Rilan area, Southeastern Desert, Egypt. In *Proceedings of the conference on 30 years of international cooperation on the geology of Egypt and related sciences* (p. 188). Special Publication No. 69.

Reich, M., Kesler, S. E., Utsunomiya, S., Palenik, C. S., Chryssoulis, S. L., & Ewing, R. C. (2005). Solubility of gold in arsenian pyrite. *Geochimica et Cosmochim Acta, 69*(11), 2781–2796.

Ringwood, A. E. (1955). The principles governing trace element distribution during magmatic crystallization. *Geochimica et Cosmochimica Acta, 7*(189–202), 242–254.

Rose, A. W., Hawkes, H. E., & Webb, J. S. (1979). *Geochemistry in mineral exploration* (2nd ed.). London, New York: Academic Press, Ltd.

Routhier, P. (1963). Les gisements metaliferes. *Geologie et Principes de Recherches, I*, 277–310. Masson et cie.

Sabet, A. H., Khalifa, K. A., Khalid, A. M., Arnous, M. M., Hassan, S. M., Abdel Daim, A. M., et al. (1983). Results of prospecting-exploration, work carried out at Um Qareiyat gold-ore deposits, Southeastern Desert, Egypt. Geol. Surv. Egypt (Internal Report).

Smirnov, V. I., Ginzburg, A. I., Grigoriev, V. M., & Yakovlev, G. F. (1983). *Studies of mineral deposits*. Moscow: Mir Publishers.

Szadeczky-Kardoss, E. (1955). *Geochemistry*. Budapest: Akademiai Kiado.

Tauson, L. V. (1961). *The geochemistry of rare elements occurring in granitoids*. Moscow: Academy of Sciences. (in Russian).

Tripathi, V. S. (1979). Factor analysis in geochemical exploration. *Journal of Geochemical Exploration, 11*, 263–275.

Turekian, K. K., & Wedepohl, K. H. (1961). Distribution of the elements in some major units of the Earth's crust. *Geological Society of America Bulletin, 72*, 175–191.

Vinogradov, A. P. (1962). Average occurrences of chemical elements in the main magmatic rock-formations of the Earth's crust. *Geokhimiya, 1962*, 555–572. (in Russian).